This is the Post-print version of the following article: *I.E. Orozco Hinostroza, M. Avalos-Borja, V.D. Compeán García, C. Cuellar Zamora, A.G. Rodríguez, E. López Luna, M.A. Vidal, Tuning emission in violet, blue, green and red in cubic GaN/InGaN/GaN quantum wells, Journal of Crystal Growth, Volume 435, 2016, Pages 110-113,* which has been published in final form at: https://doi.org/10.1016/j.jcrysgro.2015.11.022

© 2016. This manuscript version is made available under the Creative Commons Attribution-NonCommercial-NoDerivatives 4.0 International (CC BY-NC-ND 4.0) license http://creativecommons.org/licenses/by-nc-nd/4.0/

Author's Accepted Manuscript

www.elsevier.com/locate/jcrysgro

Tuning emission in violet, blue, green and red in cubic GaN/InGaN/GaN quantum wells

I.E. Orozco Hinostroza, V.D. Compeán García, C. Cuellar Zamora, A.G. Rodríguez, E. López Luna, M.A. Vidal

PII: S0022-0248(15)00690-9
DOI: http://dx.doi.org/10.1016/j.jcrysgro.2015.11.022
Reference: CRYS23071

To appear in: *Journal of Crystal Growth*

Received date: 9 October 2015
Revised date: 18 November 2015
Accepted date: 25 November 2015

Cite this article as: I.E. Orozco Hinostroza, V.D. Compeán García, C. Cuella Zamora, A.G. Rodríguez, E. López Luna and M.A. Vidal, Tuning emission ir violet, blue, green and red in cubic GaN/InGaN/GaN quantum wells, *Journal c Crystal Growth,* http://dx.doi.org/10.1016/j.jcrysgro.2015.11.022

This is a PDF file of an unedited manuscript that has been accepted fo publication. As a service to our customers we are providing this early version o the manuscript. The manuscript will undergo copyediting, typesetting, an review of the resulting galley proof before it is published in its final citable forn Please note that during the production process errors may be discovered whic could affect the content, and all legal disclaimers that apply to the journal pertain

Tuning emission in violet, blue, green and red in cubic GaN/InGaN/GaN quantum wells

I. E. Orozco Hinostroza[b], V. D. Compeán García[a] , C. Cuellar Zamora[b], A. G. Rodríguez[a], E. López Luna[a] and M. A. Vidal[a]

a) Coordinación para la Innovación y Aplicación de la Ciencia y Tecnología (CIACyT),Universidad Autónoma de San Luis Potosí (UASLP), Álvaro Obregón 64, 78000 San Luis Potosí, México

b) Instituto Potosino de Investigación Científica y Tecnológica, Camino a la Presa San José 2055,
Col. Lomas 4a Sección, 78216 San Luis Potosí, México

Accepted manuscript

ABSTRACT

Light emission in the three primary colors was achieved in cubic GaN/InGaN/GaN heterostructures grown by molecular beam epitaxy on MgO substrates in a single growth process. A heterostructure with four quantum wells with a width of 10 nm was grown; this quantum wells width decrease the segregation effect of In. Photoluminescence emission produced four different emission signals: violet, blue, green-yellow and red. Thus, we were able to tune energy transitions in the visible spectrum modifying the In concentration in cubic $In_xGa_{1-x}N$ ternary alloy.

Keywords: Single A3. Quantum wells; A3. Molecular beam epitaxy; B2. Semiconducting III-V materials; B3. Heterojunction semiconductor devices

Electronic mail: b) mavidalborbolla@yahoo.com.mx b) ignacio.orozco@ipicyt.edu.mx

ACCEPTED MANUSCRIPT

1. Introduction

In the past decades, nitride semiconductors have been used to fabricate electronic and optoelectronic devices [1-17]. Among the most important applications is solid-state lighting. Using α-GaN and α-InGaN it was possible to build a blue light-emitting diode (LED) [1]. Since this major breakthrough, the development of methods to improve growing conditions has brought remarkable results in light emitting devices [2-6]. Theoretically, due to band gap energy values of α-GaN (3.4eV) and α-InN (0.7eV), the ternary InGaN alloy can be used to cover the electromagnetic spectrum from UV to near infrared. Growing conditions that result in more than a 30% concentration of In may lead to high defect density because of the large lattice mismatch between GaN and InN (11%). Furthermore, high indium content leads to a strong quantum confinement stark effect, which reduces the radiative recombination efficiency of carriers and hinders the long wavelength range transitions. Recent reports have studied the optimization of green-yellow emission in hexagonal InGaN-based devices [3-5]. Nonetheless, red wavelength transitions with planar InGaN heterostructures remain difficult to obtain. Thus, to produce white light emitting diodes, a blue or UV LED is covered with a phosphor, which absorbs the light and reemits it with a longer wavelength. However, using phosphors such as Ce^{3+}:$Y_3Al_5O_{12}$ (one of the most common phosphors) reduces the long-term reliability and lifetime of the device [6]. Different approaches have been made to overcome this issue. One of them is to synthesize quantum wells by varying the In mole fraction in the active layer to obtain the long wavelength emission without phosphors [7]. Another approach to produce white light is to use the structures such as quantum dots in wells [8], dots in wires [9], nanorods [10], nanopyramids [11] and other nanostructures [12]. Typically, these nitride semiconductors crystallize into a hexagonal phase. Therefore, most of the previous work is based on the InGaN wurtzite phase. Nevertheless, the cubic phase has some advantages over the hexagonal phase, such as the lack of spontaneous and piezoelectric polarization [9]. Moreover, β-GaN has a lower band gap energy (3.28 eV) than α-GaN. Thus, low energy emissions in the ternary β-InGaN alloy can be obtained with a smaller In concentration than in α-InGaN.

Although it is more difficult to synthesize InGaN and GaN cubic films, it has been possible to grow them using the Metal-Organic Chemical Vapor Deposition (MOCVD), Metal-Organic Vapor Phase Epitaxy and Molecular Beam Epitaxy (MBE) techniques on the 3C-SiC, GaAs, MgO and,

Accepted manuscript

ACCEPTED MANUSCRIPT

recently, on microstructured silicon substrates [13]. Taniyasu *et al*. [14] grew β-InGaN QWs on GaAs using MOVPE that emitted in the violet-blue spectral region. Chichibu *et al*. [15] obtained violet, blue and green emissions with β-InGaN MQWs on 3C-SiC substrates using MBE. Li *et al*. [16] demonstrated green emission from β-InGaN QWs that were grown on 3C-SiC using MBE. Stark *et al*. [13] grew InGaN QWs on the v-grooved Si using MOVPE, and the device exhibited green emission. Different wavelength emissions in cubic heterostructures have been analyzed, but emissions in the blue to red region in a single structure have not been reported.

In this work, we characterize the cubic GaN/$In_xGa_{1-x}N$/GaN/ QWs that were grown using plasma assisted molecular beam epitaxy (PA-MBE) with the aim to obtain emissions in the violet, blue, green and red ranges in a single heterostructure by changing the In concentration.

2. Experimental details

All samples were grown on MgO (100) substrates to induce the cubic phase. Prior to the growing process, the substrate was degreased in trichloroethylene at 50°C for 10 min. Then, the substrate was ultrasonically cleaned in acetone and deionized water baths (10 minutes each). After that, the substrate was introduced into a vacuum loading chamber (~1×10^{-6} Torr). Then, it was transferred to the growing chamber, where it was thermally cleaned in a high vacuum environment (~3×10^{-8} Torr) at 900°C for 30 min to obtain an atomically flat surface. Because the cleaning process produces a MgO-H surface [18], the sample is exposed to atomic nitrogen for 10 min to replace H atoms with N atoms, which is more energetically favorable.

The high purity (99.9999%) solid sources were used to supply the indium and gallium fluxes, while a radio frequency (RF) plasma source was used to generate atomic nitrogen. Both β-GaN and the films were grown with a constant N_2 flow at a rate of 1.3 standard cubic centimeters per minute (sccm) and the RF power of 230 W.

Three separated SQWs were synthesized as follows. First, a 300 nm thick buffer layer was grown on the MgO substrate at 770°C. Next, a β-$In_XGa_{1-X}N$ layer with a thickness of approximately 4 ± 2 nm was deposited on three different samples using In concentrations of x=0.10, 0.40 and 0.47. Then, a 150 nm wide β-GaN barrier was grown on top (Fig. 2(d)).

The In segregation is a problem because the elevated temperature used to obtain the InGaN in cubic phase; if we used a lower temperature a hexagonal phase is induced. Therefore the typical

Accepted manuscript

ACCEPTED MANUSCRIPT

growth of ternary alloy β-$In_XGa_{1-X}N$ is 750 – 790 °C and to diminish the In segregation effect the individual quantum wells were growth for a given thickness around 4 nm.

In the next step, four β-InGaN quantum wells at different In concentration with β-GaN barriers were grown. First, a 300 nm thick β-GaN buffer layer was grown at 770°C using an epitaxial layer-by-layer growth mode. Then, four 10 ± 2 nm thick $In_xGa_{1-x}N$ layers with GaN barriers were deposited using different In concentrations. This was achieved by adjusting the indium effusion cell temperature to produce concentrations of 11%, 17%, 35% and 47% for each QW. The barriers were grown at 770°C with 50 nm for the first three samples and with a 150 nm thickness for the last sample. The reason we chose a 10 nm thickness of the well is because indium segregation is more difficult to control in a narrow QW when the growth time is longer as is the case for multiple quantum wells. Additionally, we were interested in producing three primary colors using different thicknesses. Details of the samples are summarized in table I.
A 12kV acceleration voltage was utilized in Reflection High Energy Electron Diffraction (RHEED) to determine lattice constants of the samples. Then, we applied Vegard's law to estimate the In molar fraction.

The PL emission spectra studies were carried out by mounting the samples in a cold finger of a closed-cycle cryostat and cooling them to 10 K. A He-Cd laser operating at 325 nm was used as an excitation source with an output power of 1 mW. The PL signal from the samples was analyzed using a 50 cm monochromator and was captured using a charge-coupled device (CCD).

Table I

Concentration of In, thickness and PL signal of the four grown samples.

	Concentration of In (± 2%)	Thickness (± 2 nm)	PL signal (± 0.10 eV)
Sample 1	10	4	3.08
Sample 2	40	3	2.32
Sample 3	46	4	1.92
Sample 4(4QWs)	11,17,35 and 47	10 (each QW)	2.92, 2.71, 2.07 and 1.79

Accepted manuscript

ACCEPTED MANUSCRIPT

3. Results and discussion

3.1 Single quantum well with different Indium concentrations.

Fig. 1 shows the optical band gap vs. In concentration for bulk InGaN alloys at 300 K (dashed blue line), which has been previously experimentally determined [18]. In addition to the band gap data of InN mentioned in the reference Damian *et al* [18] other experimental and theoretical data values have been published [19-21].

Because the energy band gap shifts to high values when the temperature is lowered, we estimated an average blue shift of 47 meV for the β-InGaN bulk according to Varshni fits from the PL measurements from β-GaN (80 meV) [22] and β-InN (14 meV) [23]. The solid black and orange lines observed in Fig. 1 result from infinite quantum well approximations for 3 nm and 4 nm, respectively. The β-$In_xGa_{1-x}N$ effective masses were interpolated using parameters for *β-GaN* and *β-InN* according to reference [24]. The values from the PL measurements at 10 K of samples 1 and 3 (blue squares), lie on the 4 nm curve, while the sample 2 value lies on the 3 nm curve, which is 1 nm less than the expected thickness.

Ternary alloy β-$In_xGa_{1-x}N$ layers with 3 or 4 nm thickness are almost completely relaxed because the critical thickness of GaN and InN in cubic phase are 3 and 4 monolayers as was experimentally obtained from RHEED measurements (25,26). Therefore, the ternary alloy between GaN and InN should have a similar critical thickness. In both references, a completely relaxed layer is found around 10 or 12 ML (2.2 or 2.5 nm). The only possible source of stress in these samples is due to the small thermal expansion difference between GaN and InGaN.

The Fig. 2 depicts the PL spectra for sample 1 (a), sample 2 (b) and sample 3 (c). In Fig. 2(a), a wide peak is observed, which is formed by the GaN (3.24 eV) and QW (3.08 eV) signals, with a FWHM of 0.34 eV. In Fig. 2(b), a peak at approximately 2.32 eV is seen with a FWHM of 0.35 eV. Fig. 2(c) depicts the PL with a signal observed at 1.92 eV and a FWHM of 0.35 eV. All peak positions are at higher energies compared with the bulk band gap due to the confinement effect.

3.2 Several quantum wells with different In concentrations

The intensity profile obtained from the RHEED patterns is shown in Fig. 1(a). Thus, we correlate the substrate lattice constant and the distance between rods to calculate the grown layer lattice

Accepted manuscript

parameter. The intensity profile in Fig. 3(b) shows the diffraction distance variation between bars $(\bar{1}0)$ and (10) from the sample 4 RHEED pattern during growth. The MgO (red line) profile is observe on top. For the InGaN layers (blue lines) we observe distance shrinking between bars as indium concentration increases due to larger lattice parameter. All GaN barriers have the same lattice constant (0.45 nm). In Fig. 3(b), we observe the buffer layer and final barrier profiles (black lines).

Fig. 4 shows the sample 4 photoluminescence with four principal emissions at 1.79, 2.07, 2.71 and 2.92 eV from the InGaN QWs and another emission at 3.26 eV from GaN. These QWs were wider than SQWs, therefore, less indium segregation occurred during growth. A smaller FWHM of the peaks was obtained: 0.2, 0.26, 0.43, and 0.31 eV for the wells and 0.12 for GaN. According to the concentration, which was calculated using the lattice constant estimated from RHEED (Fig. 3) and Vegard's law (equation 2) with a bowing parameter *b* of 1.4, the bulk energy gaps of alloys are 2.79, 2.57, 2.0 and 1.67 eV.

$$E_{g,InGaN} = xE_{g,InN} + (1-x)E_{g,GaN} - bx(1-x) \qquad (2)$$

Accepted manuscript

Because quantum wells are confined, the PL emission appears at higher energies compared with the bulk. Fig. 1 shows a dotted magenta line that corresponds to a 10 nm QW approximation. The green triangles were plotted with the PL energy value of each peak vs. the In concentration calculated from RHEED. The PL peak broadening is attributed to recombination from confined states inside the QWs [27] and to possible alloy fluctuations.

4. Conclusions

In summary, individual QWs were grown using cubic ternary alloys of InGaN. By controlling the growth parameters, different concentrations of In were used to tune the emitting signal in the visible electromagnetic spectrum. Thereby, a heterostructure formed of four quantum wells of GaN/InGaN/GaN in cubic phase was obtained. The violet, blue, yellow and red color emissions were observed in the PL spectrum. This was achieved by varying only the In molar concentration during a single growth process. We managed to grow β-InGaN films using MBE with high In

ACCEPTED MANUSCRIPT

concentrations, which is necessary for generating long wavelength emissions without phosphorous for possible light emitting diode applications or heterostructures to solar cells.

Acknowledgements

This work was partially supported by Consejo Nacional de Ciencia y Tecnología (CONACyT) through Grant 152155 and by CEMIE Sol 22, Mexico. The authors thank Gladis Judith Labrada Delgado for her technical support.

Accepted manuscript

References

[1] S. Nakamura, M. Senoh, and T. Mukai, Jpn. J. Appl. Phys. **32**, L8 (1993).

[2] Sung-Nam Lee, H. S. Paek, H. Kim, T. Jang, and Y. Park, Appl. Phys. Lett. **92**, 081107 (2008).

[3] C. Du, Z. Ma, J. Zhou, T. Lu, Y. Jiang, P. Zuo, H. Jia and H. Chen, Appl. Phys. Lett. **105** 071108 (2014).

[4] J. Yang , T. Wei, Q. Hu, Z. Huo, B. Sun, R. Duan and J. Wang, Mater. Sci. Semicond. Proc. **29** p. 357 (2015).

[5] Y. Jiang, Y. Li, Y. Li, Z. Deng, T. Lu, Z. Ma, P. Zuo, L. Dai, L. Wang, H. Jia, W. Wang, J. Zhou, W. Liu & H. Chen, Scientific reports, **5** (2015).

[6] R. Zhang, H. Lin, Y.L. Yu, D.Q. Chen, J. Xu and Y.S. Wang, Laser Photonics Rev. **8**, p. 158 (2014) .

[7] H. Li, P. Li, J. Kang, Z. Li, Z. Li, J. Li, X. Yi, and G. Wang, Appl. Phys. Express **6**, 102103 (2013).

[8] S.J. Chua, C.B. Soh, W. Liu, J.H. Teng, S.S. Ang, S.L. Teo, Phys. Stat. Sol. (c) **5**, 2189 (2008).

[9] H.F. Trung Nguyen, Q. Wang and Z. Mi J. Elec. Mat. Vol **43** No 4 (2014).

[10] H.-W. Lin, Y.-J. Lu, H.-Y. Chen, H.-M. Lee, and S. Gwo, Appl. Phys. Lett. **97**, 073101 (2010).

Accepted manuscript

[11] K. Wu, T. Wei, H. Zheng, D. Lan, X. Wei, Q. Hu, H. Lu, J. Wuang, Y. Luo and J. Li, J. Appl. Phys. **115**, 123101 (2014).

[12] C. B. Soh, W. Liu, A. M. Yong, S. J. Chua, S. Y. Chow, S. Tripathy, and R. J. N. Tan, Nanoscale Res. Lett. **5**, 1788 (2010).

[13] C. J. Stark, T. Detchprohm, S. C. Lee, Y. B. Jiang, S. R. J. Brueck, and C Wetzel, Appl. Phys. Lett. **103**, 232107 (2013).

[14] Y. Taniyasu, K. Suzuki, D. H. Lim, A. W. Jia, M. Shimotomai, Y. Kato and K. Takahashi, Phys. Stat. Sol. (a) **180**, 241 (2000).

[15] S. F. Chichibu, T. Onuma, T. Sota, S.P. DenBaars, S. Nakamura, T. Kitamura, Y. Ishida and H. Okumura, J. Appl. Phys. **93**, 2051 (2003).

[16] S. F. Li, J. Schörmann, D. J. As and K. Lischka, Appl. Phys. Lett. **90**, 071903 (2007).

[17] V. K. Lazarov, R. Plass, H-C. Poon, D. K. Saldin, M. Weinert, S. A. Chambers, and M. Gajdardziska-Josifovska, Phys. Rev. B **71** 115434 (2005).

[18] V.D. Compeán García, I.E. Orozco Hinostroza, A. Escobosa Echavarría, E. López Luna, A.G. Rodríguez, M.A. Vidal J. Cryst. Growth **418** 120-125 (2015).

[19] T. Inoue, Y. Iwahashi, S. Oishi, M. Oihara, Y.Hijikata, H. Yaguchi, and S. Yoshida, Phys Stat. Sol. (c) 5 1579-1581 (2008).

[20] P. Rinke, M. Schefler, A. Qteish, M. Winkelnkemper, D. Bimberg, J. Neugebauer, Appl. Phys. Letts. 89 161919 (2006).

[21] F. Bechstedt, J. Furthuller, M. Ferhat, L.K. Teles, L.M.R. Scolfaro, J.R. Leite, V. Yu Davydorv, O. Ambacher and R. Godhahm. Phys Stat. Sol. (a) 195, 628-633 (2008).

Accepted manuscript

[22] G. Ramírez-Flores, H. Navarro-Contreras, A. Lastras-Martínez, R. C. Powell, and J. E. Greene Phys. Rev. B **50**, 8433 (1994).

[23] M. Pérez-Caro, A. G. Rodríguez, M. A. Vidal, and H. Navarro-Contreras J. Appl. Phys. **108**, 013507 (2010).

[24] [21] H. Morcoç, Handbook of Nitride Semiconductors and Devices vol. 1 (Wiley-VCH, New York) (2008).

[25] M. Pérez Caro, Alfredo Mejía, A.G. Rodríguez, H. Navarro-Contreras, M.A. Vidal, J. Crystal Grwoth 311 1302-1305 (2009).

[26] M. Pérz Caro, A.G. Rodríguez, E. López-Luna, M.A. Vidal, H. Navarro-Contreras, J. Appl. Phys. 107, 083510 (2010).

[27] S. C. P. Rodrigues, G. M. Sipahi, L. M. R. Scolfaro, O. C. Noriega, J. R. Leite, T. Frey, D. J. As, D. Schikora, and K. Lischka Phys. Stat. Sol. (a) **190**, No. 1, 121–127 (2002).

Accepted manuscript

ACCEPTED MANUSCRIPT

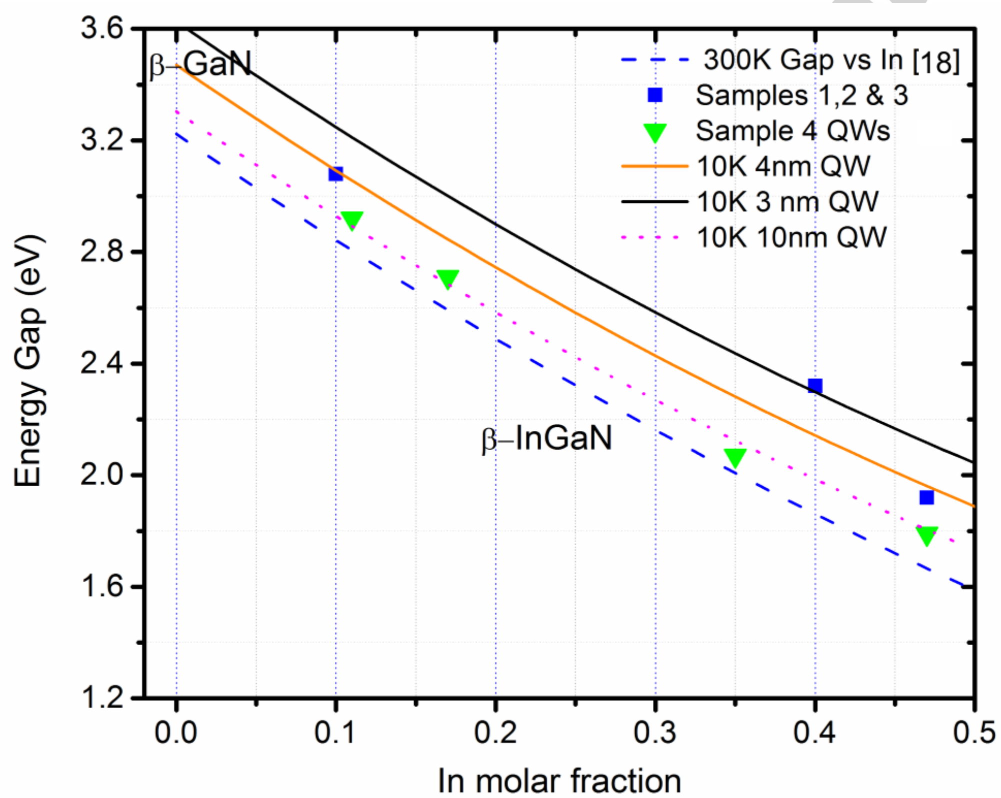

FIG. 1. Energy gap vs. In molar fraction for InGaN alloys in bulk. The blue squares correspond to emission of InGaN QWs for three different In concentrations.

ACCEPTED MANUSCRIPT

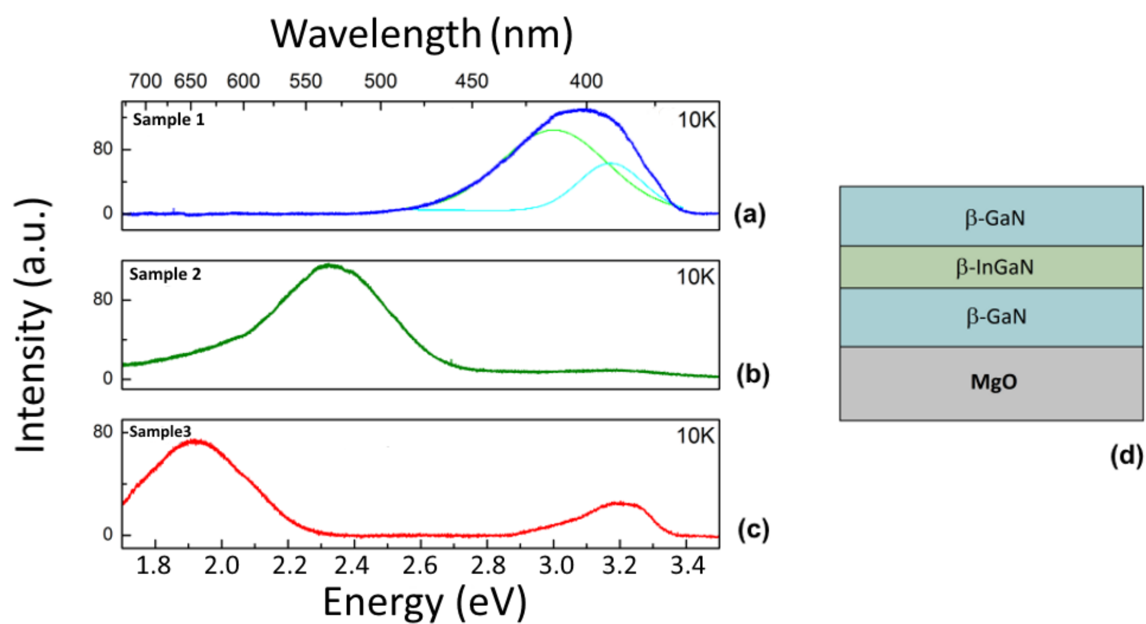

FIG. 2. Photoluminescence of InGaN SQWs with In concentration of x = 0.10 (a), x = 0.40 (b), and x = 0.47 (c). Schematic diagram of the SQWs (d)

Accepted manuscript

ACCEPTED MANUSCRIPT

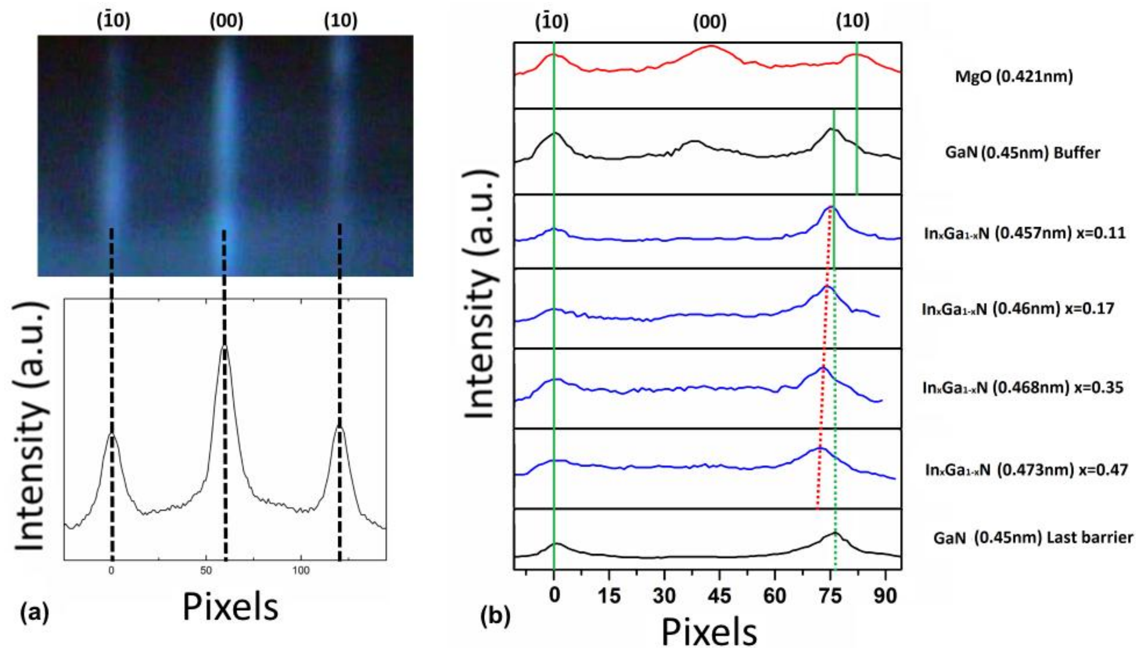

FIG. 3. RHEED intensity profiles along the [110] azimuth. a) Example of a substrate pattern and its profile. b) Distance changes between bars $(\bar{1}0)$ and (10) during the growth of sample 4.

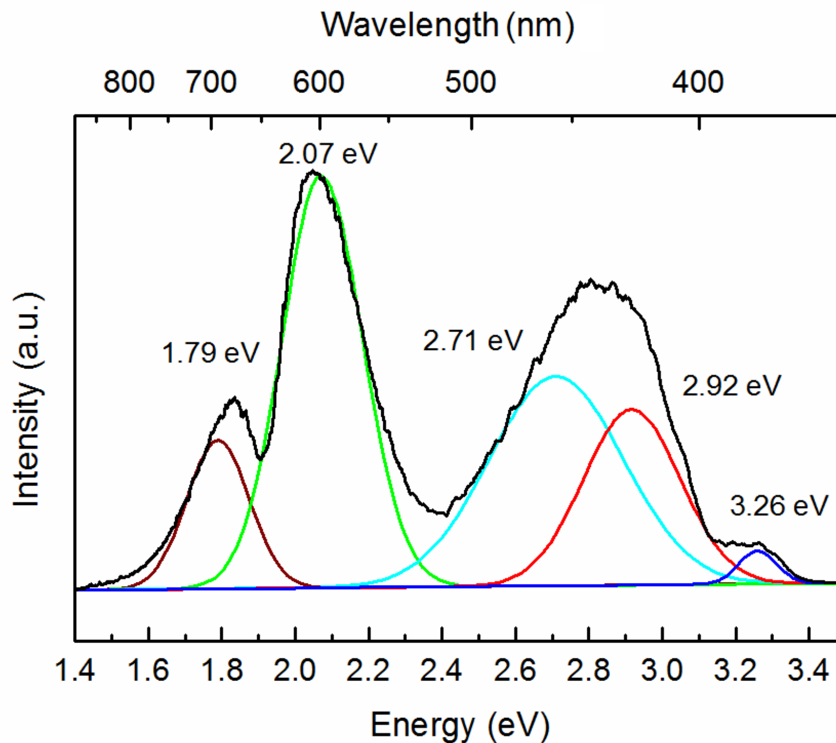

FIG. 4. Sample 4 photoluminescence at 10K. A fitting of 5 peaks is shown, which includes the GaN signal at 3.26 eV.

ACCEPTED MANUSCRIPT

Table I

Concentration of In, thickness and PL signal of the four grown samples.

	Concentration of In (± 2%)	Thickness (± 2 nm)	PL signal (± 0.10 eV)
Sample 1	10	4	3.08
Sample 2	40	3	2.32
Sample 3	46	4	1.92
Sample 4(4QWs)	11,17,35 and 47	10 (each QW)	2.92, 2.71, 2.07 and 1.79

Accepted manuscript

ACCEPTED MANUSCRIPT

Highlights:
A3. Quantum wells;
A3. Molecular beam epitaxy;
B2. Semiconducting III-V materials; (InGaN in cubic phase)
B3. Heterojunction semiconductor devices

Accepted manuscript